Title

Engineered bacteria detect tumor DNA.

Journal

Science (New York, N.Y.), 381(6658)

ISSN

0036-8075

Authors

Cooper, Robert M

Wright, Josephine A

Ng, Jia Q

et al.

Publication Date

2023-08-01

DOI

10.1126/science.adf3974

Engineered bacteria detect tumor DNA

Robert M. Cooper[1*], Josephine A. Wright[2*], Jia Q. Ng[3], Jarrad M. Goyne[2], Nobumi Suzuki[2,3], Young K. Lee[3], Mari Ichinose[2,3], Georgette Radford[3], Feargal J. Ryan[2,4], Shalni Kumar[5], Elaine M. Thomas[3], Laura Vrbanac[3], Rob Knight[6,7,8,9], Susan L. Woods[2,3†], Daniel L. Worthley[2,10†] and Jeff Hasty[1,5,6,9†].

1. Synthetic Biology Institute, University of California, San Diego, La Jolla, CA, USA, 92093.
2. Precision Cancer Medicine Theme, South Australia Health and Medical Research Institute, Adelaide, SA, Australia, 5000.
3. Adelaide Medical School, University of Adelaide, Adelaide, SA, Australia, 5000.
4. Flinders Health and Medical Research Institute, Flinders University, Bedford Park, SA, Australia, 5042.
5. Department of Bioengineering, University of California, San Diego, La Jolla, CA, 92093
6. Molecular Biology Section, Division of Biological Sciences, University of California, San Diego, La Jolla, CA, USA, 92093
7. Department of Pediatrics, University of California, San Diego, La Jolla, CA, 92093
8. Department of Computer Science & Engineering, University of California, San Diego, La Jolla, CA, 92093.
9. Center for Microbiome Innovation, University of California, San Diego, La Jolla, CA, 92093
10. Colonoscopy Clinic, Brisbane, QLD, Australia, 4000

[*] contributed equally.

[†] corresponding authors.

Word count:

Abstract = 112 words

The main text (abstract plus body text) = 2066 words

Abstract

Synthetic biology has developed sophisticated cellular biosensors to detect and respond to human disease. However, biosensors have not yet been engineered to detect specific extracellular DNA sequences and mutations. Here, we engineered naturally competent *Acinetobacter baylyi* to detect donor DNA from the genomes of colorectal cancer (CRC) cells, organoids, and tumors. We characterized the functionality of the biosensors in vitro with co-culture assays and then validate in vivo with sensor bacteria delivered to mice harboring colorectal tumors. We observe horizontal gene transfer from the tumor to the sensor bacteria in our mouse model of CRC. This Cellular Assay for Targeted, CRISPR-discriminated Horizontal gene transfer (CATCH) enables the biodetection of specific cell-free DNA.

Main text

Bacterial engineering has allowed the development of living cell diagnostics and therapeutics (*1–3*), including microbes that respond to gut inflammation (*4*), intestinal bleeding (*5*), pathogens (*6*) and hypoxic tumors (*7*). Bacteria can access the entire gastrointestinal tract to produce outputs measured in stool (*4*) or urine (*7*). Cellular memory, such as bistable switches (*4*, *8*, *9*) or genomic rearrangements (*10*), enables bacteria to store information over time. Some bacteria are naturally competent for transformation and can sample extracellular DNA directly from their environment (*11*). Natural competence is one mechanism of horizontal gene transfer (HGT), the exchange of genetic material between organisms outside vertical, "parent to offspring", transmission (*12*). HGT is common between microbes (*12*). It may also occur from microbes into animals and plants (*13*) and, in the opposite direction, from eukaryotes to prokaryotes (*14*). The forward engineering of bacteria to detect and respond to mammalian DNA via HGT, however, has not been explored.

Acinetobacter baylyi is a highly competent and well-studied bacterium (*15*, *16*) that is largely non-pathogenic in healthy humans (*17*), can colonize the murine gastrointestinal tract (*18*), and acquires unpurified, environmental DNA from lysed cells (*19*). Our CATCH strategy delivers bacterial biosensors to sample and genomically integrate target DNA (Fig. 1). To demonstrate this concept, we use the biosensor to detect engineered tumor cells. We then develop genetic circuits to detect natural, non-engineered tumor DNA sequences, discriminating oncogenic mutations at the single base level. Since the target sequence and output gene are modular, our approach can be generalized to detect arbitrary DNA sequences and respond in a programmable manner.

Results

Engineering cancer cell lines, organoids and sensor bacteria

To test the hypothesis that bacteria could detect specific mammalian DNA, we generated transgenic donor human cancer cells with a kanamycin resistance gene (*kanR*) inside *KRAS* homology arms (Figs. 1, 2A-C, S1, S2). *KRAS* is an important oncogene in human cancer, and

a driver mutation in *KRAS* often accompanies the progression of simple into advanced colorectal adenomas (*20*). Our technology is currently confined to the detection of specific sequences and thus for cancer detection is limited to hotspot mutations, such as *KRASG12D.* We stably transduced this donor cassette into 3 conventional human CRC cell lines with differing background genetic alterations (RKO is microsatellite instability high, MSI-H, *BRAFV600E;* LS174T is MSI-H, *KRASG12D;* SW620 is microsatellite stable, MSS, *KRASG12V*) and two human CRC organoid lines (RAH057T is MSS, *KRASG12D;* RAH038T is MSI-H, *BRAFV600E*) using a lentiviral vector. To construct the sensor bacteria, we inserted a complementary landing pad with *KRAS* homology arms into *A. baylyi*. We tested both a "large insert" design, where 2 kb of donor cassette must transfer (Fig. 2A & B, S2A, data file S1), and a "small insert" design where only 8 bp must transfer to repair 2 stop codons (Fig. 2C, S2B, supplementary materials and methods)(*21*). The initial biosensor output was growth on kanamycin plates (Fig. 2 and Fig S2).

Detection of cell-free DNA from cancer cell lines.

We tested these designs using various donor DNA sources, both in liquid culture and on solid agar (Fig. 2A). The "large insert" biosensors detected donor DNA from purified plasmids and genomic DNA both in liquid (Fig. 2D) and on agar (Fig. 2E). On agar, they also detected raw, unpurified lysate, albeit at just above the limit of detection (Fig. 2E). As expected (*22*), the "small insert" design improved detection efficiency approximately 10-fold, reliably detecting even raw lysate (Fig. 2F-G, Movie S1). Across conditions, detection on solid agar was more efficient than in liquid culture. Importantly, these experiments confirmed that the biosensors did not require DNA purification (*19*).

Mutations in codon 12 of *KRAS* occur in 27% of CRC (*23*), accounting for 72% of all CRC *KRAS* mutations (*24*), and are common in solid tumors generally (*25*). To test whether sensor bacteria could discriminate between wild-type and mutant *KRAS (KRASG12D)*, we utilized *A. baylyi's* endogenous Type I-F CRISPR-Cas system (*26*). We stably transduced a donor RKO cell line with the *kanR-GFP* donor cassette flanked by wild-type *KRAS*, and a second line with *KRASG12D* flanking sequences. Next, we designed three CRISPR spacers targeting the wild-type *KRAS* sequence at the location of the *KRASG12D* mutation, using the *A. baylyi* protospacer-adjacent motif (PAM) (Fig. 2H). We inserted these as single-spacer arrays into a neutral locus in the "large insert" *A. baylyi* sensor genome.

The sensor bacteria should reject wild-type *KRAS* through CRISPR-mediated DNA degradation but allow integration of the *KRASG12D* sequence. Two of the three spacers blocked transformation by both wild-type and mutant DNA (Fig. 2I-J). However, spacer 2, for which the *KRASG12D* mutation eliminated the PAM site, selectively permitted only *KRASG12D* donor DNA (Fig. 2I-J). The other common mutations in codon 12 of *KRAS* all eliminate this PAM as well (*23*). Thus, sensor *A. baylyi* can be engineered to detect a mutational hotspot in the *KRAS* gene with single-base specificity.

Detection of cell-free DNA from tumorigenic organoid lines.

Next, we evaluated our sensor and donor constructs in organoid culture (Fig. 3A). We previously used CRISPR/Cas9 genome engineering to generate compound *Braf*^{V600E}*; Tgfbr2*$^{\Delta/\Delta}$*; Rnf43*$^{\Delta/\Delta}$*; Znrf3*$^{\Delta/\Delta}$*; p16Ink4a*$^{\Delta/\Delta}$ (BTRZI) mouse organoids that recapitulate serrated CRC when injected into the mouse colon (*27*). We transduced BTRZI organoids with the donor DNA construct to generate donor CRC organoids and incubated their lysate with the more efficient "small insert" *A. baylyi* biosensors. Using qPCR we confirmed that the BTRZI organoids we generated contained only 2 copies of the target donor DNA (Fig. S3). As with the CRC cell lines, the sensor *A. baylyi* incorporated DNA from donor organoid lysate, but not from control lysates from the parental organoids (Figs. 3B, S4 & S5A). Next, we co-cultured GFP-expressing sensor *A. baylyi* with parental or donor organoids for 24 hours on Matrigel. The GFP-expressing sensor bacteria enveloped the organoids (Fig. 3C). Following co-culture with donor, but not parental, organoids, the *A. baylyi* sensor bacteria acquired donor DNA via HGT (Figs. 3D, S5B & C). Finally, we estimated the detection limit of our biosensor for target DNA in stool. To achieve this, we added increasing amounts of donor plasmid to a defined mixture of biosensor and stool (5 x10^7 biosensor mixed with 0.017 g/100 µl stool slurry). The detection limit was 3 pg of plasmid or 2.7x10^5 copies of target DNA, for a given incubation volume and time (Fig. S6).

Detection of cell-free tumor DNA in an orthotopic mouse model of colorectal cancer.
Given that cancer-to-bacterial HGT occurred in vitro, and in the presence of stool, we sought to test the CATCH system in vivo. We first confirmed that our BTRZI, orthotopic CRC model released tumoral DNA into the colorectal lumen. Engineered CRC organoids were injected orthotopically, by mouse colonoscopy, into the mouse colon to form colonic tumors, as previously described (*27*). Using digital droplet PCR, we measured *Braf* mutant tumor DNA in stools collected from tumor-bearing and control mice. The BTRZI model reliably released tumor DNA into the colorectal lumen (Fig. S7).

We next conducted an orthotopic CRC experiment (Fig. 3E). NSG mice were injected with donor or non-donor organoids, or neither. At week 5, once the tumors had grown into the lumen, sensor (or parental) *A. baylyi* bacteria were delivered twice via rectal enema. The mice were subsequently euthanized and the colorectum harvested with the luminal effluent plated for analysis. Serial dilutions were then plated on agar with different antibiotic combinations (Fig 3F).

HGT from tumors to biosensors was only detected in donor tumor-bearing mice that were administered sensor bacteria. There was no HGT detected in any control group (Fig. 3F). The resistant colonies were confirmed to be the engineered biosensor strain by antibiotic resistance, green fluorescence, 16S sequencing, and HGT-mediated *kanR* repair of individual colonies (Fig. S8). Thus, CATCH discriminated mice with and without CRC in our experimental model (Fig. 3G).

Detection of non-engineered DNA.
Finally, we designed living biosensors to detect and analyze non-engineered cancer DNA. The *tetR* repressor gene was inserted between the *KRAS* homology arms in the biosensor, and in a

second locus, we placed an output gene under control of the P_LtetO-1 promoter (*28*) (Fig. 4A). Here, the output gene was kanamycin resistance for ease of measurement, but the output gene is arbitrary and exchangeable.

In this design, expression of the output gene is constitutively repressed (Fig. 4A). Upon recombination with the *KRAS* target DNA, the repressor *tetR* is deleted from the genome. If the incoming *KRAS* sequence is wild type at the G12 locus, Cascade, the Type I-F CRISPR-Cas effector complex, detects and degrades it (Fig. 4B). However, if the G12 locus is mutated, the PAM site and therefore CRISPR-Cas targeting are eliminated, and expression from the output gene turns on (Fig. 4C).

We tested this natural DNA sensor design in vitro using PCR products from LS174T and RKO genomes as donor DNA. Natural DNA biosensors with a random CRISPR spacer detected DNA sequences from both cell lines (Fig. 4D), and biosensors with the *KRAS* spacer accurately detected only DNA sequence from LS174T cells, which contain the *KRASG12D* mutation (Fig. 4E), demonstrating biosensor detection and discrimination of natural target DNA.

Discussion

The sensor bacteria described here demonstrate that a living biosensor can detect specific mammalian DNA shed from CRC in vivo in the gut, with no sample preparation or processing. Engineered donor cassettes are not required for CATCH biosensors to detect, discriminate, and report on target sequences, although the final natural DNA biosensors will need an improved signal-to-background ratio to reliably detect sequences within whole genomic DNA. The homology arms and CRISPR spacers are modular, so this strategy could be readily adapted to detect and analyze arbitrary target sequences of interest.

Our technology is not yet ready for clinical application. This approach requires further development to ensure that future versions, at least those designed for gastrointestinal use, may be delivered orally and achieve sufficient luminal density to allow reliable detection by non-invasive sampling such as in stool or blood. As the technology advances towards clinical care, we will also need to more critically evaluate the performance of CATCH compared to other relevant disease-specific tests such as, in this case, colonoscopy and in vitro nucleic acid assays (*29*, *30*). There is also further bioengineering required to limit the risk of biosensors escaping circuit-mediated cell death and to improve the efficiency of natural DNA detection. Finally, as our technology progresses, careful analysis is essential to ensure patient safety, to minimize the risk of spreading antibiotic resistance and to satisfy biocontainment concerns. These necessary next steps are being actively pursued and are important as CATCH is applied to additional preclinical models and before it is trialed in humans.

In vitro DNA analysis helps detect and manage important human diseases, including cancer and infection (*31*). However, in vitro sensing requires potentially invasive removal of samples, and many DNA diagnostics do not achieve clinically relevant sequence resolution, with more advanced techniques remaining too expensive for routine use in all settings (*32*). Direct

sampling of the gut in vivo may offer important advantages. The gastrointestinal tract contains marked DNase activity (*33*), which limits the lifetime of free DNA in both rodents and humans (*18*, *34*, *35*), and may thus reduce the information content of downstream fecal samples. Bacterial biosensors located in situ could capture and preserve DNA shortly after its release before degradation by local DNases. Perhaps the most exciting aspect of CATCH, however, is that unlike in vitro diagnostics, once target DNA is captured, it could be coupled to direct and genotype-complementary delivery of nanobodies, peptides, or other small molecules for the treatment of cancer or infection (*36*, *37*). CATCH allows for the cellular detection of cell-free DNA and thus may prove useful in future synthetic biology applications, wherever, and whenever, DNA detection and analysis is important.

References and notes

1. S. Slomovic, K. Pardee, J. J. Collins, Synthetic biology devices for in vitro and in vivo diagnostics. *Proc National Acad Sci*. 112, 14429–14435 (2015).

2. F. Sedlmayer, D. Aubel, M. Fussenegger, Synthetic gene circuits for the detection, elimination and prevention of disease. *Nat Biomed Eng*. 2, 399–415 (2018).

3. W. A. Lim, C. H. June, The Principles of Engineering Immune Cells to Treat Cancer. *Cell*. 168, 724–740 (2017).

4. D. T. Riglar, T. W. Giessen, M. Baym, S. J. Kerns, M. J. Niederhuber, R. T. Bronson, J. W. Kotula, G. K. Gerber, J. C. Way, P. A. Silver, Engineered bacteria can function in the mammalian gut long-term as live diagnostics of inflammation. *Nat Biotechnol*. 35, 653–658 (2017).

5. M. Mark, N. Phillip, H. Alison, C. Sean, F. Sarah, J. Logan, C. Joy, M. Shane, S. Richard, C. J. Robert, B. Vladimir, L. Robert, T. Giovanni, C. P. Anantha, L. K. Timothy, An ingestible bacterial-electronic system to monitor gastrointestinal health. *Science*. 360, 915 (2018).

6. N. Mao, A. Cubillos-Ruiz, D. E. Cameron, J. J. Collins, Probiotic strains detect and suppress cholera in mice. *Sci Transl Med*. 10, eaao2586 (2018).

7. T. Danino, A. Prindle, G. A. Kwong, M. Skalak, H. Li, K. Allen, J. Hasty, S. N. Bhatia, Programmable probiotics for detection of cancer in urine. *Sci Transl Med*. 7, 289ra84-289ra84 (2015).

8. J. W. Kotula, S. J. Kerns, L. A. Shaket, L. Siraj, J. J. Collins, J. C. Way, P. A. Silver, Programmable bacteria detect and record an environmental signal in the mammalian gut. *Proc National Acad Sci*. 111, 4838–4843 (2014).

9. T. S. Gardner, C. R. Cantor, J. J. Collins, Construction of a genetic toggle switch in Escherichia coli. *Nature*. 403, 339–342 (2000).

10. A. Courbet, D. Endy, E. Renard, F. Molina, J. Bonnet, Detection of pathological biomarkers in human clinical samples via amplifying genetic switches and logic gates. *Sci Transl Med*. 7, 289ra83 (2015).

11. M. Chang Joshua, R. J Rosemary, Natural competence and the evolution of DNA uptake specificity. *J Bacteriol*. 196, 1471–1483 (2014).

12. S. M. Soucy, J. Huang, J. P. Gogarten, Horizontal gene transfer: building the web of life. *Nature Reviews Genetics*. 16, 472–482 (2015).

13. K. M. Robinson, K. B. Sieber, J. C. D. Hotopp, A Review of Bacteria-Animal Lateral Gene Transfer May Inform Our Understanding of Diseases like Cancer. *Plos Genet*. 9, e1003877 (2013).

14. J. C. D. Hotopp, Horizontal gene transfer between bacteria and animals. *Trends Genet*. 27, 157–163 (2011).

15. D. M. Young, D. Parke, L. N. Ornston, Opportunities for genetic investigation afforded by Acinetobacter baylyi, a nutritionally versatile bacterial species that is highly competent for natural transformation. *Annu Rev Microbiol*. 59, 519–551 (2005).

16. R. Palmen, B. Vosman, P. Buijsman, C. K. D. Breek, K. J. Hellingwerf, Physiological characterization of natural transformation in Acinetobacter calcoaceticus. *Microbiology+*. 139, 295–305 (1993).

17. T.-L. Chen, L.-K. Siu, Y.-T. Lee, C.-P. Chen, L.-Y. Huang, R. C.-C. Wu, W.-L. Cho, C.-P. Fung, Acinetobacter baylyi as a Pathogen for Opportunistic Infection ▿ . *J Clin Microbiol*. 46, 2938–2944 (2008).

18. L. Nordgård, T. Nguyen, T. Midtvedt, Y. Benno, T. Traavik, K. M. Nielsen, Lack of detectable DNA uptake by bacterial gut isolates grown in vitro and by Acinetobacter baylyi colonizing rodents in vivo. *Environmental Biosafety Research*. 6, 149–160 (2007).

19. R. M. Cooper, L. Tsimring, J. Hasty, Inter-species population dynamics enhance microbial horizontal gene transfer and spread of antibiotic resistance. *eLife*. 6, 8053 (2017).

20. B. Vogelstein, E. R. Fearon, S. R. Hamilton, S. E. Kern, A. C. Preisinger, M. Leppert, Y. Nakamura, R. White, A. M. Smits, J. L. Bos, Genetic Alterations during Colorectal-Tumor Development. *New Engl J Medicine*. 319, 525–532 (1988).

21. See supplementary materials.

22. D. J. Simpson, L. F. Dawson, J. C. Fry, H. J. Rogers, M. J. Day, Influence of flanking homology and insert size on the transformation frequency of Acinetobacter baylyi BD413. *Environmental Biosafety Research*. 6, 55–69 (2007).

23. AACR Project GENIE Consortium, AACR Project GENIE: Powering Precision Medicine through an International Consortium. *Cancer Discov*. 7, 818–831 (2017).

24. W. Li, Y. Liu, S. Cai, C. Yang, Z. Lin, L. Zhou, L. Liu, X. Cheng, W. Zeng, Not all mutations of KRAS predict poor prognosis in patients with colorectal cancer. *Int J Clin Exp Patho*. 12, 957–967 (2018).

25. P. Priestley, J. Baber, M. P. Lolkema, N. Steeghs, E. de Bruijn, C. Shale, K. Duyvesteyn, S. Haidari, A. van Hoeck, W. Onstenk, P. Roepman, M. Voda, H. J. Bloemendal, V. C. G. Tjan-Heijnen, C. M. L. van Herpen, M. Labots, P. O. Witteveen, E. F. Smit, S. Sleijfer, E. E. Voest, E. Cuppen, Pan-cancer whole-genome analyses of metastatic solid tumours. *Nature*. 575, 210–216 (2019).

26. R. M. Cooper, J. Hasty, One-Day Construction of Multiplex Arrays to Harness Natural CRISPR-Cas Systems. *Acs Synth Biol*. 9, 1129–1137 (2020).

27. T. R. M. Lannagan, Y. K. Lee, T. Wang, J. Roper, M. L. Bettington, L. Fennell, L. Vrbanac, L. Jonavicius, R. Somashekar, K. Gieniec, M. Yang, J. Q. Ng, N. Suzuki, M.

Ichinose, J. A. Wright, H. Kobayashi, T. L. Putoczki, Y. Hayakawa, S. J. Leedham, H. E. Abud, Ö. H. Yilmaz, J. Marker, S. Klebe, P. Wirapati, S. Mukherjee, S. Tejpar, B. A. Leggett, V. L. J. Whitehall, D. L. Worthley, S. L. Woods, Genetic editing of colonic organoids provides a molecularly distinct and orthotopic preclinical model of serrated carcinogenesis. *Gut*. 68, 684–692 (2018).

28. R. Lutz, H. Bujard, Independent and tight regulation of transcriptional units in Escherichia coli via the LacR/O, the TetR/O and AraC/I1-I2 regulatory elements. *Nucleic Acids Research*. 25, 1203–1210 (1997).

29. C. Myhrvold, C. A. Freije, J. S. Gootenberg, O. O. Abudayyeh, H. C. Metsky, A. F. Durbin, M. J. Kellner, A. L. Tan, L. M. Paul, L. A. Parham, K. F. Garcia, K. G. Barnes, B. Chak, A. Mondini, M. L. Nogueira, S. Isern, S. F. Michael, I. Lorenzana, N. L. Yozwiak, B. L. MacInnis, I. Bosch, L. Gehrke, F. Zhang, P. C. Sabeti, Field-deployable viral diagnostics using CRISPR-Cas13. *Science*. 360, 444–448 (2018).

30. J. S. Chen, E. Ma, L. B. Harrington, M. D. Costa, X. Tian, J. M. Palefsky, J. A. Doudna, CRISPR-Cas12a target binding unleashes indiscriminate single-stranded DNase activity. *Science*. 546, eaar6245 (2018).

31. Y. Zhong, F. Xu, J. Wu, J. Schubert, M. M. Li, Application of Next Generation Sequencing in Laboratory Medicine. *Ann Lab Med*. 41, 25–43 (2021).

32. M. Iwamoto, J. Y. Huang, A. B. Cronquist, C. Medus, S. Hurd, S. Zansky, J. Dunn, A. M. Woron, N. Oosmanally, P. M. Griffin, J. Besser, O. L. Henao, C. for D. C. and P. (CDC), Bacterial enteric infections detected by culture-independent diagnostic tests--FoodNet, United States, 2012-2014. *Mmwr Morbidity Mortal Wkly Rep*. 64, 252–7 (2015).

33. O. Shimada, H. Ishikawa, H. Tosaka-Shimada, T. Yasuda, K. Kishi, S. Suzuki, Detection of Deoxyribonuclease I Along the Secretory Pathway in Paneth Cells of Human Small Intestine. *J Histochem Cytochem*. 46, 833–840 (1998).

34. A. Wilcks, A. H. A. M. van Hoek, R. G. Joosten, B. B. L. Jacobsen, H. J. M. Aarts, Persistence of DNA studied in different ex vivo and in vivo rat models simulating the human gut situation. *Food Chem Toxicol*. 42, 493–502 (2004).

35. T. Netherwood, S. M. Martín-Orúe, A. G. O'Donnell, S. Gockling, J. Graham, J. C. Mathers, H. J. Gilbert, Assessing the survival of transgenic plant DNA in the human gastrointestinal tract. *Nat Biotechnol*. 22, 204–209 (2004).

36. M. O. Din, T. Danino, A. Prindle, M. Skalak, J. Selimkhanov, K. Allen, E. Julio, E. Atolia, L. S. Tsimring, S. N. Bhatia, J. Hasty, Synchronized cycles of bacterial lysis for in vivo delivery. *Nature*. 536, 81–5 (2016).

37. G. D. Sepich-Poore, L. Zitvogel, R. Straussman, J. Hasty, J. A. Wargo, R. Knight, The microbiome and human cancer. *Science*. 371, eabc4552 (2021).

Acknowledgements: P Winning, Winning Media, for design assistance with Figure 1. Figure 2A and figure 3A created with BioRender.com. B Leggett and V Whitehall, Queensland

Institute of Medical Research, for the original gift of the parental RKO, SW620 and LS174T human CRC cell lines used in this study.

Funding: This work was supported by NIH grant R01CA241728 (JH) and NHMRC ideas grant 2020555 (DW).

Author contributions: RC, DW & JH conceived of the concept and study plan. RC, JW, JN, JG, NS, YL, MI, GR, FR, SK, ET, LV, SW, DW, & JH were all involved with data acquisition and or interpretation. RC, JW, RK, SW, DW, & JH were involved in writing and revising the final manuscript.

Competing interests: JH is a co-founder and board member of, and JH, DW and SW have equity in, GenCirq Inc, which focuses on cancer therapeutics. DW, JH and RC are inventors on a provisional patent application, "Detection of Cancer Mutations", filed by the University of California San Diego with the US Patent and Trademark Office (Application No. 63/239,100). All other authors declare that they have no competing interests.

Data and materials availability: All data are available in the manuscript or the supplementary materials. Correspondence and requests for materials should be addressed to:
Professor Jeff Hasty: hasty@ucsd.edu
Associate Professor Daniel Worthley: dan@colonoscopyclinic.com.au
Associate Professor Susan Woods: susan.woods@adelaide.edu.au

Supplementary Materials
Materials and Methods
Figs. S1 to S8
References (*38-43)*
Movie S1
Data file S1

Figure legends

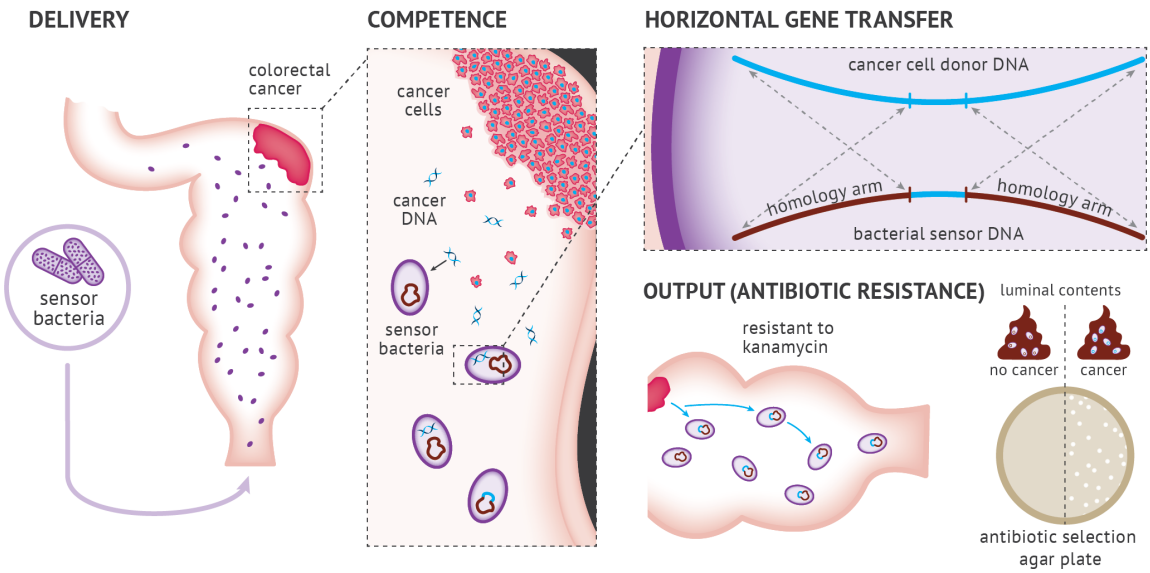

Figure 1. Engineered bacteria to detect tumor DNA. Engineered *A. baylyi* bacteria are delivered rectally in an orthotopic mouse model of CRC. The naturally competent *A. baylyi* take up tumor DNA shed into the colorectal lumen. The tumor donor DNA is engineered with a *kanR* cassette flanked by *KRAS* homology arms. The sensor bacteria are engineered with matching *KRAS* homology arms that promote homologous recombination. Sensor bacteria that undergo HGT from tumor DNA acquire kanamycin resistance and are quantified from luminal contents by serial dilution on antibiotic selection plates.

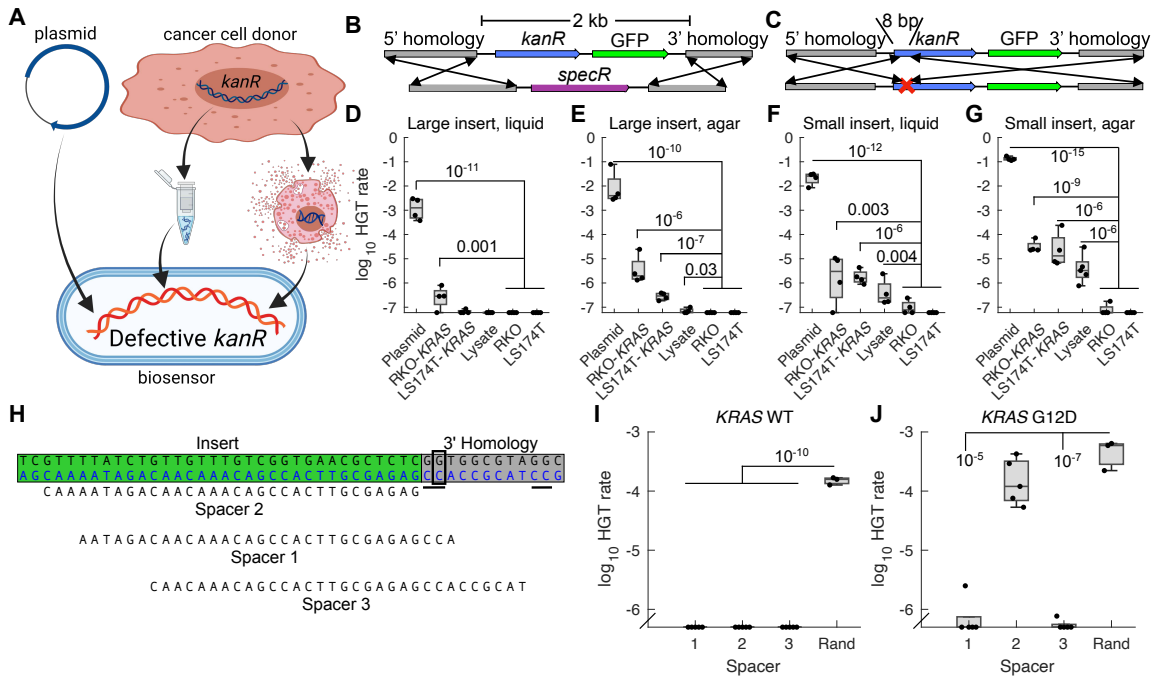

Figure 2: Sensing *KRASG12D* DNA in vitro. A, Donor DNA was derived from plasmid, purified cancer cell genomic DNA, or raw lysate (top) that recombined into biosensor *A. baylyi* cells (bottom). Horizontal gene transfer included either a large, 2 kb insert **B**, or a small, 8 bp insert to repair 2 stop codons **C,** in both cases conferring kanamycin resistance. **D-G**) *A. baylyi* biosensors were incubated with plasmid DNA, purified RKO-*KRAS* or LS174T-*KRAS* genomic DNA, or raw RKO-*KRAS* lysate, all containing the donor cassette, or purified RKO or LS174T genomic DNA as controls. Biosensor cells included either "large insert" (**B, D & E**) or "small insert" (**C, F & G**) designs, and transformations were performed in liquid culture (**D & F)** or on solid agar surfaces (**E & G**). Two sample t-tests compared data to RKO and LS174T genomic DNA controls under the same conditions. **H**, CRISPR spacers targeting the *KRAS* G12D mutation (boxed), using the underlined PAMs. Fraction of total biosensor cells expressing the indicated CRISPR spacers that were transformed by plasmid donor DNA with wild type (**I**) or mutant G12D (**J**) *KRAS*. Statistics were obtained using two sample, one-sided t-tests, with p-values displayed on the figures. Data points below detection are shown along the x-axis, at the limit of detection.

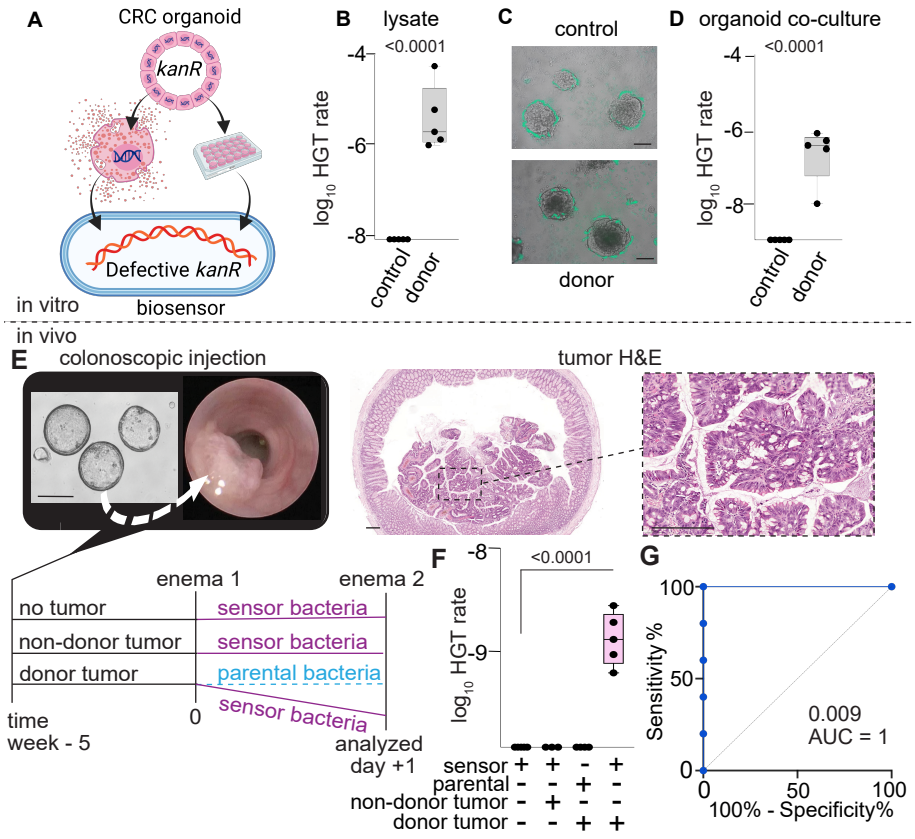

Figure 3: Detection of donor DNA from BTRZI-*KRAS-kanR* organoids in both an in vitro and an in vivo model of colorectal cancer.

A, Schema depicting in vitro co-culture of *A. baylyi* sensor bacteria with BTRZI-*KRAS-kanR* (CRC donor) organoid lysates or viable organoids to assess HGT repair of kanamycin resistance gene (*kanR*). **B**, Recombination with DNA from crude lysates enables growth of *A. baylyi* sensor on kanamycin. **C**, Representative images of GFP-tagged *A. baylyi* biosensor surrounding parental BTRZI (control) and BTRZI-*KRAS-kanR* donor organoids at 24h. Scale bar 100 µm. **D,** Co-culture of established CRC BTRZI-*KRAS-kanR* donor organoids with *A. baylyi* sensor enables growth of *A. baylyi* sensor on kanamycin. In **B & D,** n = 5 independent experiments each with 5 technical replicates, one sample t-test on transformed data was used for statistical analysis with p-values as indicated. **E,** Schema depicting in vivo HGT experiments: generation of BTRZI-*KRAS-kanR* (CRC donor) tumors in mice via colonoscopic injection, with tumor pathology validated by H&E histology, administration of biosensors, and analysis of luminal contents. Scale bars 200µm. **F,** rectal delivery of *A. baylyi* biosensor to mice bearing CRC donor tumors results in kanamycin resistant *A. baylyi* biosensor in luminal contents via HGT with transformation efficiency of $1.5x10^{-9}$ (limit of detection $1.25x10^{-10}$). HGT rate calculated from CFU on kanamycin/chloramphenicol/vancomycin (transformants) and chloramphenicol/vancomycin (total *A. baylyi*) selection plates, n=3-5 mice/group. One-way ANOVA with Tukey's post-hoc on log10 transformed data was used for statistical analysis. **G,** ROC curve analysis of HGT CFU following enema, AUC = 1, p = 0.009.

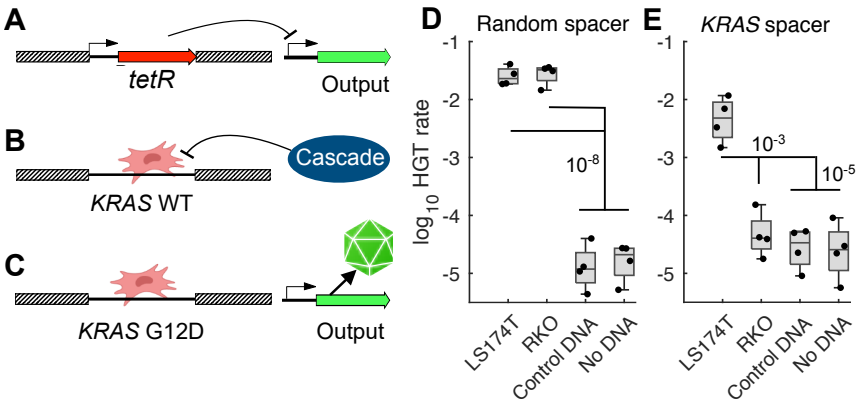

Figure 4: Detection of non-engineered DNA. A, *tetR* located between the homology arms on the *A. baylyi* genome represses expression of the output gene. **B,** Target DNA with wild-type *KRAS* sequence is recognized and degraded by the Type I-F CRISPR-Cas effector complex, Cascade. **C,** Target DNA with the *KRASG12D* mutation avoids degradation, replaces *tetR* in the biosensor genome, and relieves repression of the output gene. Fraction of biosensors with either a random CRISPR spacer **D**, or a spacer targeting wild type *KRAS* **E,** that detected donor DNA. Statistics were obtained via two sample t-tests and are displayed on the figure.

Supplementary Materials

Materials and Methods

Bacterial cell culture and cloning to generate biosensors

Acinetobacter baylyi ADP1 was obtained from the American Type Culture Collection (ATCC #33305) and propagated in standard LB medium at 30 or 37 °C. *KRAS* homology arms were inserted into a neutral genetic locus denoted *Ntrl1*, replacing the gene remnant ACIAD2826. For the "large insert" design, a spectinomycin resistance gene was placed between the *KRAS* homology arms. For the "small insert" design, two stop codons were placed near the beginning of the *kanR* gene of the donor cassette, and the broken cassette was inserted into *A. baylyi*. CRISPR arrays were inserted into a neutral locus used previously (*38*), replacing ACIAD2186, 2187, and part of 2185. Ectopic CRISPR arrays were driven by a promoter region that included 684 bp from upstream of the first repeat of the endogenous, 90-spacer array.

For natural DNA biosensors, a temperature-sensitive *tetR* repressor was placed between the *KRAS* homology arms. An output gene, either *kanR* or GFP, was placed under control of the P_LtetO-1 promoter in a second neutral locus denoted *Ntrl2*, replacing the gene remnants ACIAD1076-1077. Repeated attempts to clone wild type *tetR* into *A. baylyi* failed, but we fortuitously isolated a temperature sensitive mutant with two mutations: W75R and an additional 8 amino acids on the C terminus. This mutant *tetR* permitted growth at both 30 and 37 °C, but it only repressed its target at 30°C. The W75R mutant had been isolated previously in an intentional screen (*39*). We were able to clone wild-type *tetR* on the inducer aTc, but it was unable to grow without aTc at any temperature.

In vitro biosensor transformation experiments

A. baylyi were grown overnight in LB at 30 °C. Cells were then washed, resuspended in an equal volume of fresh LB, and mixed with donor DNA. For transformation in liquid, 50 µl cells were mixed with 250 ng donor DNA and incubated in a shaker at 30 °C for 2 hours or overnight. For transformation on agar, 2 µl cells were mixed with >50 ng donor DNA, spotted onto LB plates containing 2% wt/vol agar, and incubated at 30 °C overnight. Spots were cut out the next day and resuspended in 500 µl phosphate buffered saline solution (PBS). To count transformants, cells were 10-fold serially diluted 5 times, and 2 µl spots were deposited onto selective (30 ng/ml kanamycin) and non-selective 2% agar plates, with 3 measurement replicates at each dilution level. Larger volumes of undiluted samples were also spread onto agar plates to increase detection sensitivity (25 µl for liquid culture, 100 µl for resuspended agar spots). Colonies were counted at the lowest countable dilution level after overnight growth at 30 °C, and measurement replicates were averaged. Raw, unpurified lysate was produced by growing donor RKO cells in a culture dish until confluence, trypsinizing and harvesting cells, pelleting them in a 15 ml tube, resuspending them in 50 µl PBS, and placing the tube in a –20 °C freezer overnight to disrupt cell membranes.

In vitro statistics

Hypothesis testing was performed using two sample, one-sided t-tests in Matlab after taking base 10 logarithms, since serial dilutions produce log-scale data. Where data points were below

the limit of detection, they were replaced by the limit of detection as the most conservative way to include them in log-scale analysis. Comparisons between large vs small inserts or liquid vs solid agar culture were performed using paired t-tests, where data were matched for donor DNA and either culture type (liquid vs agar) or insert size, respectively. For Figure 2, D-G) n=4, I & J) n=5 except for random spacer n=3.

Creation of RKO, LS174T and SW620 donor cell lines

To create RKO donor and LS174T donor cell lines, lentiviral expression plasmid pD2119-FLuc2 KRasG12D donor was co-transfected with viral packaging vectors, psPAX2 (Addgene; plasmid; 12260) and MD2G (Addgene; plasmid; 12259), into HEK293T cells. At 48 and 72 h after transfection, viral supernatants were harvested, filtered through a 0.45-µm filter, and concentrated using Amicon Ultra Centrifugal Filters (Merck Millipore; UFC910024). Concentrated lentivirus particles were used for transduction. The viral supernatant generated was used to transduce RKO, LS174T and SW620 cells. 48 hours after transduction, stable transformants were selected with 4 µg/ml puromycin. Cell line identity was confirmed by STR analysis. KRAS status of RKO (*KRAS* wildtype), LS174T (*KRAS G12D*) and SW620 (*KRAS G12V*) cell lines was confirmed by amplification of a 220bp PCR fragment of the exon 2 KRAS gene, including codons 12 and 13 with primers KRAS F: GGTGGAGTATTTGATAGTGTATTAACC and KRAS R: AGAATGGTCCTGCACCAGTAA. Sanger sequencing was conducted using the same primers.

Creation of CRC donor organoids

BTRZI (*Braf^{V600E};Tgfbr2$^{\Delta/\Delta}$;Rnf43$^{\Delta/\Delta}$;Znf43$^{\Delta/\Delta}$;p16 Ink4a$^{\Delta/\Delta}$*) organoids were generated using CRISPR-Cas9 engineering and grown in 50 µl domes of GFR-Matrigel (Corning; 356231) in organoid medium: Advanced Dulbecco's modified Eagle medium/F12 (Gibco; 12634010) supplemented with 1x gentamicin/antimycotic/antibiotic (Gibco; 15710064, 15240062), 10mM HEPES (Gibco; 15630080), 2 mM GlutaMAX (Gibco; 35050061), 1x B27 (Gibco; 12504-044), 1x N2 (Gibco; 17502048), 50 ng/ml mouse recombinant EGF (Peprotech; 315-09), 10 ng/ml human recombinant TGF-β1 (Peprotech; 100-21) (*40*). Following each split, organoids were cultured in 10 µM Y-27632 (MedChemExpress; HY-10583), 3 µM iPSC (Calbiochem; 420220), 3 µM GSK-3 inhibitor (XVI, Calbiochem; 361559) for the first 3 days. Human colorectal tumor samples were obtained at the time of surgery for routine pathological analysis. All participants gave written informed consent and research was conducted in accordance with the Declaration of Helsinki, the NHMRC Statement on Ethical Conduct in Human Research, and institutional approval (HREC/16/SAC/344 SSA/18/CALHN/71). Tumor organoid lines were derived as previously described with minor modifications (*41*). Tissue samples were first minced and enzymatically digested in organoid digestion medium containing advanced DMEM-F12 (Gibco; 12634-010), Antibiotic-Antimycotic (Gibco; 15240-062), 50 µg/ml Gentamicin (Gibco; 15750-060), 1% FCS, Collagenase IV 75 U/ml (Gibco; 17104019), Dispase 125 µg/ml (Gibco; 17105-041), Hyaluronidase 20 µg/ml (Sigma; H3506), Y27632 (Sigma; Y0503) in a water bath at 37 °C for 10 minutes then a further 30 minutes shaking at 150 rpm in an orbital shaker at 37 °C. Samples were strained, washed and plated in domes of GFR-Matrigel (Corning; 356231). Human CRC organoids were cultured in colorectal

cancer medium containing advanced DMEM/F12 (Gibco; 12634-010), Antibiotic-Antimycotic (Gibco; 15240-062), 50 µg/ml Gentamicin (Gibco; 15750-060), 10 mM HEPES (Sigma; H0887), 1x glutamax (Gibco; 35050-061), 2x B27 (Gibco; 17504044), 500 nM A83–01 (Tocris; 2939), 50 ng/ml hEGF (Sigma; SRP3027), 1 nM [Leu15]-Gastrin 1 (Sigma; G9145), 1 mM N-Acetyl-Lcysteine (Sigma; A9165), 5 µM SB202190 (Sigma; S7067), 10 µM SB431542 (Sigma; S4317), and 10 µM Y27632 (Sigma; Y0503). Colorectal cancer medium was changed twice weekly, with growth monitored until passaging was required.
To create CRC donor organoids, lentiviral expression plasmid pD2119-FLuc2 *KRASG12D* donor was co-transfected with viral packaging vectors, psPAX2 (Addgene; plasmid; 12260) and MD2G (Addgene; plasmid; 12259), into HEK293T cells. At 48 and 72 h after transfection, viral supernatants were harvested, filtered through a 0.45-µm filter, and concentrated using Amicon Ultra Centrifugal Filters (Merck Millipore; UFC910024). Concentrated lentivirus particles were used for transduction. The viral supernatant generated was used to transduce human CRC and BTRZI organoids by spinoculation. Briefly, organoids were dissociated to single cells using TrypLE. $1x10^5$ single cells were mixed with 250 µl organoid medium; 10 µM Y-27632; 250 µl concentrated viral supernatant and 4 µg/ml polybrene (Sigma; H9268) in a 48 well tray before centrifugation at 600*g* for 90 minutes at 32 °C. Meanwhile, 120 µl 50:50 ADMEM:Matrigel mixture was added to a cold 24-well tray before centrifugation of this bottom Matrigel layer for 40 minutes at 200*g* at room temperature, followed by solidifying the Matrigel by incubating at 37 °C for 30 minutes. After spinoculation, cells were scraped from the well and plated on top of the Matrigel monolayer with organoid medium. The following day, the medium was removed and the upper layer of Matrigel was set over the organoids by adding 120 µl 50:50 ADMEM:Matrigel and allowing to set for 30 minutes before adding organoid medium. 48 hours after transduction, BTRZI donor organoids were selected with 8 µg/ml puromycin (Sigma; P8833) for 1 week, then maintained in organoid medium with 4 µg/ml puromycin. Human CRC donor organoids were selected and maintained in 4 µg/ml puromycin.

Calculating number of copies of target DNA integrated into cell lines and organoids
Genomic DNA (gDNA) was extracted from $5x10^6$ cells using Purelink genomic DNA minikit (Invitrogen; K18200). Primer/probe sets were designed to amplify the human KRAS homology arms within the donor construct. 5'*KRAS* homologyArm FWD 5'- CAG AAC AGC AGT CTG GCT ATT TA-3'; 5'*KRAS* homologyArm REV 5'- ACT GCA GAC GTG TAT CGT AAT G -3' and 5' *KRAS* homologyArm PRB 5'-/56-FAM/AGC GTC GAT /ZEN/GGA GGA GTT TGT AAA TGA/31ABkFQ/-3'. Quantitative PCR (qPCR) reactions were optimized with normal human gDNA (from PBMC), mouse gDNA (BTRZI parental organoid gDNA) and BTRZI donor gDNA to show that primer/probe sets amplify both endogenous human *KRAS* and the donor construct, but not mouse *Kras*. To enable calculation of copy number of each cell and organoid line, a standard curve was generated with normal human gDNA (2-fold serial dilution 100 ng to 3.125 ng per qPCR reaction). qPCR was conducted on 25 ng gDNA from organoids and cell lines. All qPCR reactions were normalized to 100 ng per qPCR reaction with mouse gDNA (BTRZI parental organoid gDNA) and used KAPA probe fast universal (Roche; KK4703).

Organoid lysate mixed with *A. baylyi* sensor bacteria

BTRZI (parental) and BTRZI donor organoids were grown for 5 days in 50 µl GFR-Matrigel domes. Organoids were dissociated to single cells with TrypLE, counted and $6x10^5$ single cells were collected in PBS and snap frozen. The CFU equivalence of exponentially growing *A. baylyi* sensor culture at OD_{600} 0.35 was ascertained by serial dilution of 3 independent cultures with 5 technical replicates plated on 10 µg/ml chloramphenicol LB agar plate to be 2.4 x 10^8 CFU per ml. *A. baylyi* sensor was grown in liquid culture with 10 µg/ml chloramphenicol to OD_{600} 0.35 before mixing with organoid lysate at a 1:1 ratio and grow overnight on LB agar plates at 30 °C. All bacteria were scraped into 200 µl LB/20% glycerol before spotting 5x 5 µl spots onto kanamycin (Sigma; K1377) and chloramphenicol (Sigma; C0378) plates and grown overnight at 37 °C. Colonies were counted and the dilution factor was accounted for to calculate CFU per ml. Rate of HGT was calculated by dividing the CFU per ml of transformants (kanamycin plates) by the CFU per of total *A. baylyi* (chloramphenicol plates) for 5 independent experiments.

Coculture organoids with *A. baylyi* sensor bacteria

For co-culture experiments, 24-well trays were coated with Matrigel monolayers. Briefly, 200 µl 50:50 ADMEM:Matrigel mixture was added to a cold 24-well tray and centrifuged for 40 minutes at 200xg at room temperature, followed by a 30-minute incubation at 37 °C to solidify Matrigel. BTRZI (parental) and BTRZI donor organoids were dissociated into small clusters using TrypLE and grown for 5 days on a Matrigel monolayer in organoid medium without antibiotics before 50 µl OD_{600} 0.35 *A. baylyi* sensor was added to each well. After 24 hours, organoids were photographed then collected and grown overnight on LB agar plates at 30 °C. All bacteria were scraped into 200 µl LB/20% glycerol before spotting 5x 5 µl spots onto kanamycin and chloramphenicol plates and grown overnight at 37 °C. Colonies were counted and the dilution factor was accounted for to calculate CFU per ml. Rate of HGT was calculated by dividing the CFU per ml of transformants (kanamycin plates) by the CFU per ml of total *A. baylyi* (chloramphenicol plates) for 5 independent experiments.

Horizontal gene transfer in vivo

BTRZI donor organoids were isolated from Matrigel and dissociated into small clusters using TrypLE. The cell clusters (equivalent to ~150 organoids per injection) were washed three times with cold PBS containing 10 µM Y-27632 and then resuspended in 20 µl 10% GFR Matrigel 1:1000 Indian ink, 10 µM Y-27632 in PBS and orthotopically injected into the mucosa of the proximal and distal colon of anaesthetized 10- to 13-week-old NSG mice (150 organoids per injection), as previously described *(40).* Briefly, a customized needle (Hamilton Inc. part number 7803-05, removable needle, 33 gauge, 12 inches long, point 4, 12° bevel) was used. In each mouse up to 2 injections of 20µl were performed. CRC donor tumor growth was monitored by colonoscopy for 5 weeks and the videos were viewed offline using QuickTime Player for analysis. Colonoscopy was performed using a Karl Storz Image 1 Camera System comprised of: Image1 HDTV HUB CCU; Cold Light Fountain LED Nova 150 light source; Full HD Image1 3 Chip H3-Z Camera Head; Hopkins Telescope, 1.9mm, 0 degrees. A sealed Luer Lock was placed on the working channel of the telescope sheath to ensure minimal air leakage (Coherent Scientific; 14034-40). Tumor growth of the largest tumor visualized was

scored as previously described using the Becker Scale (*42*). All study groups were housed in separate cages. *A. baylyi* sensor was grown in LB liquid culture with 6 µg/ml chloramphenicol to OD_{600} 0.6. *A. baylyi* parental was grown in LB liquid culture to OD_{600} 0.6. *A. baylyi* was washed twice with PBS before 13 mice received $4x10^{10}$ *A. baylyi* sensor via enema (5 mice without tumors; 3 mice with non-donor BTRZI CRC tumors and 5 mice with BTRZI CRC donor tumors), 4 mice received $4x10^{10}$ *A. baylyi* parental via enema. Enema was performed as per previous publication *(43)*. Briefly, mice were anesthetized with isoflurane and colon flushed with 1 ml of room temperature sterile PBS to clear the colon cavity of any remaining stool. A P200 pipette tip coated with warm water was then inserted parallel into the lumen to deliver 50 µl of bacteria into the colon over the course of 30 seconds. After infusion, the anal verge was sealed with Vetbond Tissue Adhesive (3M; 1469SB) to prevent luminal contents from being immediately excreted. Animals were maintained on anesthesia for 5 minutes, and then allowed to recover on heat mat and anal canal inspected 6 hours after the procedure to make sure that the adhesive has been degraded. 24 hours after *A. baylyi* administration, mice received a second enema dosing. Mice were then euthanized; colons were removed and luminal contents were collected. Luminal contents were grown overnight at 37 °C on LB agar with 10 µg/ml vancomycin plates. All bacteria were collected into 250 µl LB/20% glycerol, vortexed and stored at -80 °C. 5x 5µl serial dilutions were spotted onto LB agar plates containing: 1, vancomycin (to detect total *A. baylyi* parental); 2, chloramphenicol; vancomycin (to detect total *A. baylyi* sensor) and 3, kanamycin; chloramphenicol; vancomycin (to detect recombined *A. baylyi* sensor). Colonies were counted and dilutions were factored to calculate CFU *A. baylyi* per mouse. For experiments analyzing *A. baylyi* in stool, BTRZI CRC donor tumors were established and monitored as described above. After 5 weeks of tumor growth, 9 mice received *A. baylyi* sensor enemas (5 mice without tumors; 4 mice with BTRZI CRC donor tumors) and 6 mice received *A. baylyi* parental enemas (3 mice without tumors and 3 mice with BTRZI CRC donor tumors). Stool was collected 24 hours after *A. baylyi* administration into 250 µl PBS/20% glycerol, vortexed and stored at -80 °C. Stool was analyzed on LB agar plates containing: 1, vancomycin (Sigma; PHR1732) (to detect total *A. baylyi* parental); 2, chloramphenicol; vancomycin (to detect total *A. baylyi* sensor) and 3, kanamycin; chloramphenicol; vancomycin (to detect recombined *A. baylyi* sensor). Colonies were counted and dilutions were factored to calculate CFU *A. baylyi* per mouse.

Sequencing gDNA from bacterial colonies grown on kanamycin plates

A. baylyi transformants were individually picked from kanamycin; vancomycin plates and grown in liquid culture LB supplemented with 25 µg/ml kanamycin, 10 µg/ml vancomycin and 6 µg/ml chloramphenicol. gDNA was extracted using purelink genomic DNA minikit (Invitrogen; K182001). Genomic regions of interest were amplified using Primestar Max DNA polymerase (Takara; R045A) and primers HGTpcrF: CAAAATCGGCTCCGTCGATACTA; HGTpcrR: TAGCATCACCTTCACCCTC and 16S 27Fa: AGAGTTTGATC**A**TGGCTCAG; 16s 27Fc: AGAGTTTGATC**C**TGGCTCAG; 16S 1492R: CGGTTACCTTGTTACGACTT (16S 27Fa:16S 27Fc: 16S 1492R = 0.5:0.5:1). Sanger sequencing was conducted using the same primers.

Calculating the detection limit of CATCH in the presence of stool

Stools were collected from C57BL/6 mice bearing CRC tumors. A stool slurry was created by vortexing 10 mouse stools (average weight 0.017 g) in 830 µl LB/20% glycerol for each experiment, then 100 µl stool slurry could be added to each reaction containing the equivalent of 1 stool. Donor plasmid DNA was serially diluted (10-fold from 3 ng/µl to 30 fg/µl). *A. baylyi* sensor was grown in LB liquid culture with 6 µg/ml chloramphenicol to OD600 0.6. 5 x10^7 *A. baylyi* sensor was mixed with 100 µl stool slurry or 100 µl LB/20% glycerol with or without serially diluted donor plasmid DNA. Reactions were incubated at 37°C for 4 hours before serially diluting (10-fold) and spotting 5x 5 µl spots onto 25 µg/ml kanamycin; 10 µg/ml vancomycin LB agar plates and 6 µg/ml chloramphenicol; 10 µg/ml vancomycin LB agar plates and grown overnight at 37 °C. Colonies were counted and the dilution factor was accounted for to calculate CFU per ml. Rate of HGT was calculated by dividing the CFU per ml of transformants (kanamycin plates) by the CFU per ml of total *A. baylyi* (chloramphenicol plates) for 5 independent experiments.

Supplementary figures

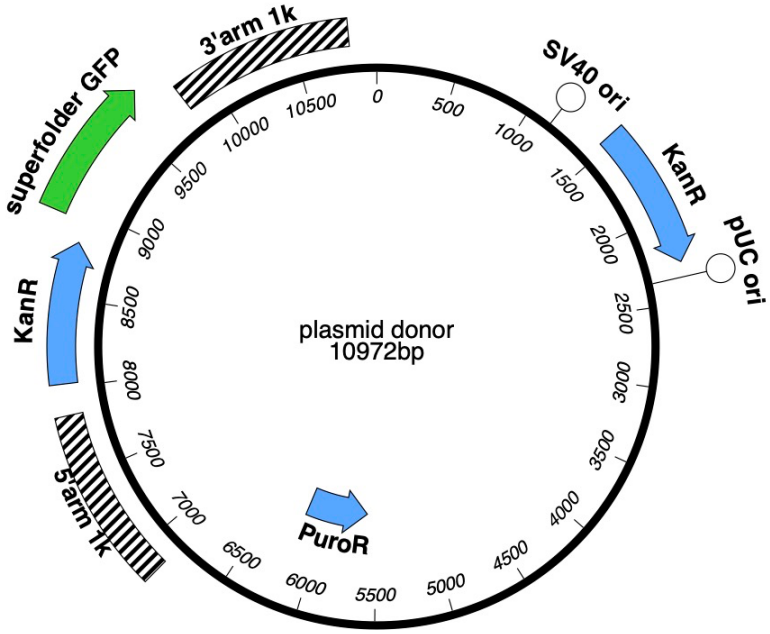

Figure S1: Engineered donor construct. Plasmid donor DNA used to transfect mammalian cell lines and as positive control donor DNA for in vitro experiments.

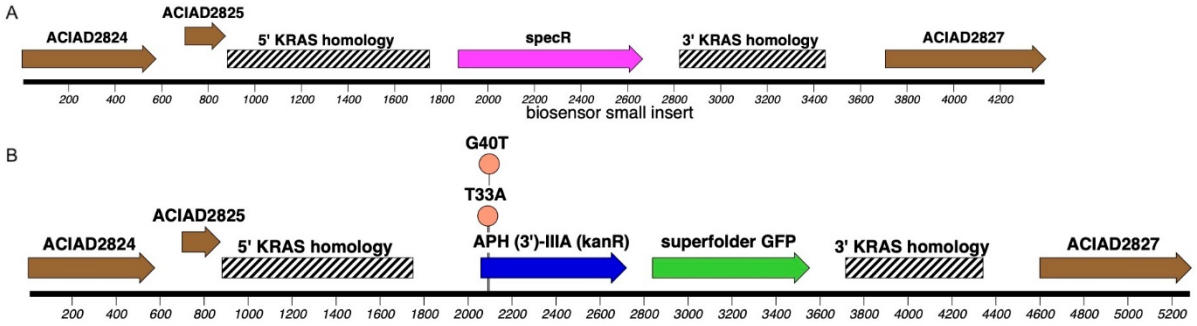

Figure S2: Engineered landing pad within the biosensor to receive target DNA. "Large insert" **A**, and "small insert" **B**, designs for the biosensors. *KRAS* homology arms are shown in striped, gray with surrounding genomic context outside them. Note that large and small inserts refer to the size of the donor DNA region that must transfer to confer kanamycin resistance, not to the size of the region between homology arms in the biosensor. Two single-base changes introducing nearby stop codons at the beginning of *kanR* are shown for the small insert design, **B**.

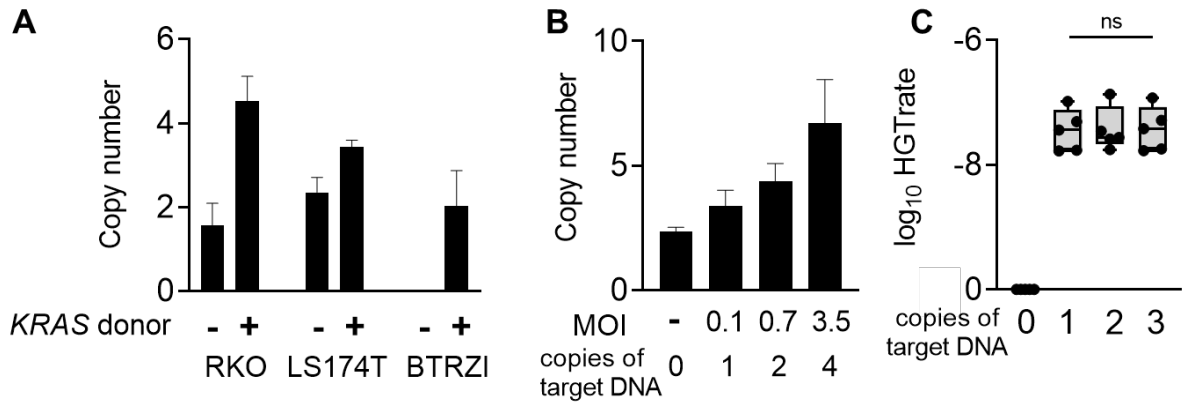

Figure S3: Copy number of target DNA within cancer cell and organoid lines. A, on average 1 to 3 copies of target donor DNA were integrated per cell into polyclonal donor cell and organoid lines. The number of copies of target donor DNA integrated per cell was quantitated using qPCR with primers designed to amplify the KRAS homology arms in the donor cassette, as well as endogenous human KRAS. Parental RKO and LS174T cell lines were diploid for human KRAS (2n), whereas human KRAS could not be amplified from parental BTRZI mouse organoid genomic DNA. Donor cells had endogenous KRAS locus (2n) as well as 2.5±0.6 (RKO) and 1.4±0.2 (LS174T) copies of target donor DNA. BTRZI donor organoids had 2.0±0.8 copies of target donor DNA (mouse endogenous KRAS locus not detectable by human specific primers). n=3 independent gDNA extractions per sample with each qPCR conducted in triplicate and compared to a standard curve generated with normal human gDNA. **B**, LS174T cells were transduced with different multiplicity of infection (MOI) and stable cell lines were selected with 2 μg/ml puromycin. Donor cells had endogenous KRAS locus (2n) and 1.4 (MOI0.1), 2.4 (MOI0.7) and 4.7 (MOI3.5) copies of target donor DNA. **C**, Recombination with donor DNA from crude lysates of LS174T donor cell lines, with different numbers of target donor DNA integrated per cell, enables growth of *A. baylyi* sensor on kanamycin plates. n=5 independent experiments each with 5 technical replicates. Paired t-test showed that there was no significant difference in recombination efficiency.

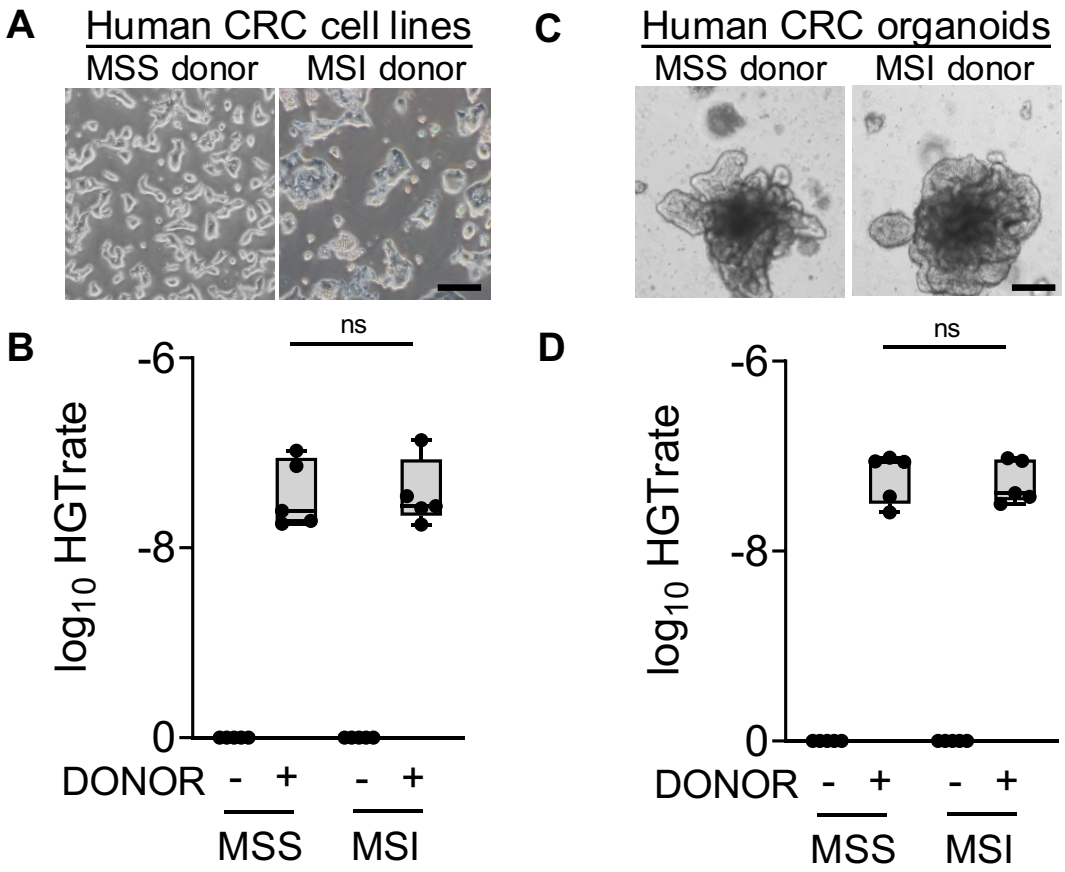

Figure S4: Detection of donor DNA from both MSS and MSI colorectal cell lines and human organoids. A, Images of human CRC cell lines, SW620 (MSS) and LS174T (MSI-H), with the donor cassette stably integrated into their genome. Scale bar 200 μm. **B**, Recombination with DNA from crude lysates of human CRC donor cell lines enables growth of *A. baylyi* sensor on kanamycin plates. **C**, Images of human CRC organoids established from patient surgical samples with the donor cassette stably integrated into their genome. Scale bar 200 μm. **D**, Recombination with DNA from crude lysates of human CRC donor organoid lines enables growth of *A. baylyi* sensor on kanamycin plates. In b and d, n=5 independent experiments each with 5 technical replicates. Paired t-test showed that there was no significant difference in recombination efficiency between MSS and MSI patient organoids.

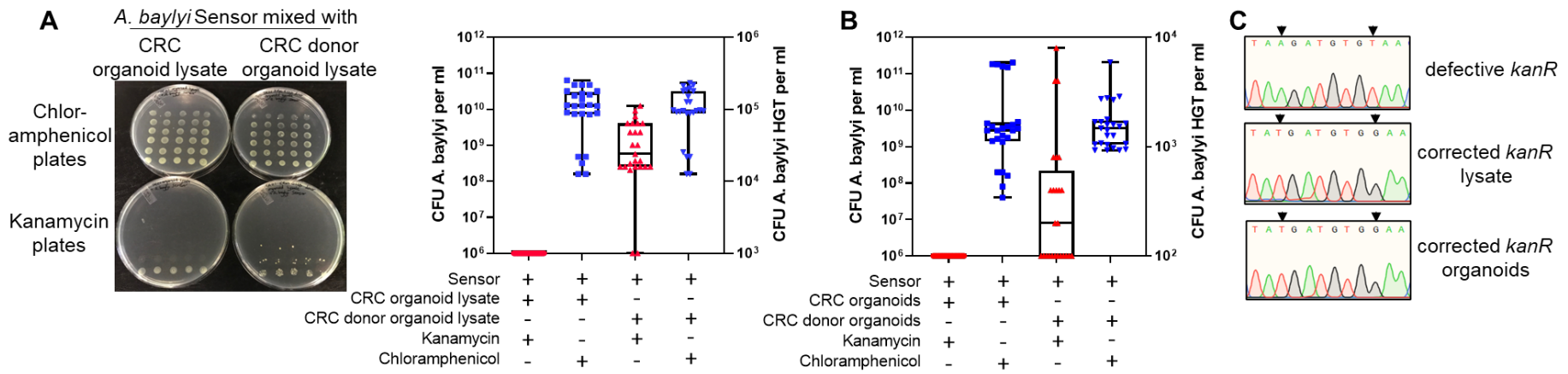

Figure S5: Sensor detection of donor DNA from BTRZI CRC organoids. *A. baylyi* sensor bacteria are constitutively chloramphenicol-resistant, hence c*hlorR* CFUs provide a readout of total *A. baylyi* present. In contrast, kanamycin-resistant sensor bacteria rely on incorporation of donor DNA from CRC organoids to correct the defective *kanR* gene and enable growth on kanamycin selection plates. **A,** Recombination with lysate from CRC donor organoids enables growth of *A. baylyi* sensor on kanamycin plates. Shown here with representative plates and CFU analysis. **B,** after co-culturing established CRC donor organoids with *A. baylyi* sensor, recombination with donor DNA from CRC donor organoids enables growth of *A. baylyi* sensor on kanamycin plates. Shown here with representative images and CFU analysis. Scale bars 200 µm. **A & B,** Fig 3 contains the same data as shown here but presented as HGT rate (kanamycin resistant CFU *A. baylyi* per ml/chloramphenicol CFU *A. baylyi* per ml*),* n = 5 independent experiments each with 5 technical replicates. **C** Representative Sanger sequencing chromatograms of PCR amplicon covering the region of the *kanR* gene containing informative SNPs, to highlight the difference in sequence in gDNA isolated from parental *A. baylyi* sensor bacteria compared to *A. baylyi* colonies isolated from kanamycin plates following mixing with donor organoid lysates or viable organoids.

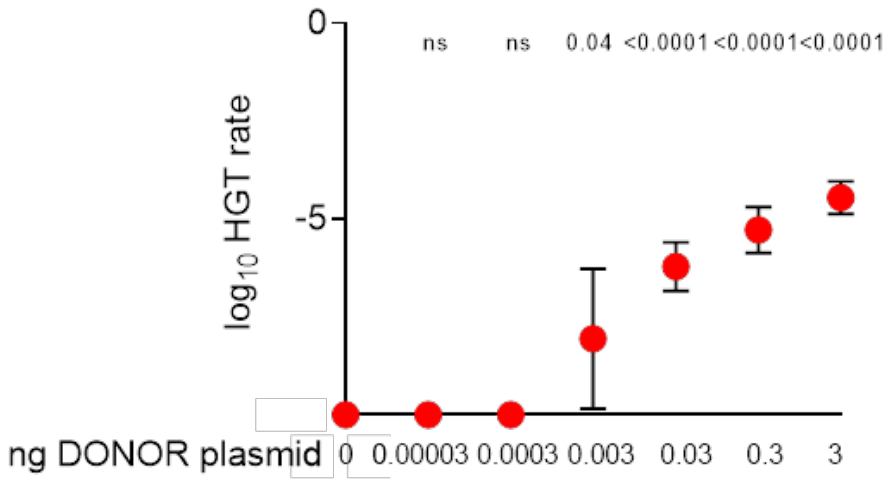

Figure S6: Detection of target DNA mixed with stool. *A. baylyi* sensor bacteria were mixed with serially diluted donor plasmid DNA in the presence of mouse stool collected from mice bearing CRC tumors (1 stool per reaction). After 3 hours of growth at 37 °C, serial dilutions of each reaction were plated onto kanamycin/vancomycin LB agar selection plates (*A. baylyi* sensor HGT) or chloramphenicol/vancomycin LB agar selection plates (total *A. baylyi* sensor). Rate of HGT was calculated (p-values calculated on log-transformed data using unpaired t-test). n=5 independent experiments, each with 5 technical replicates.

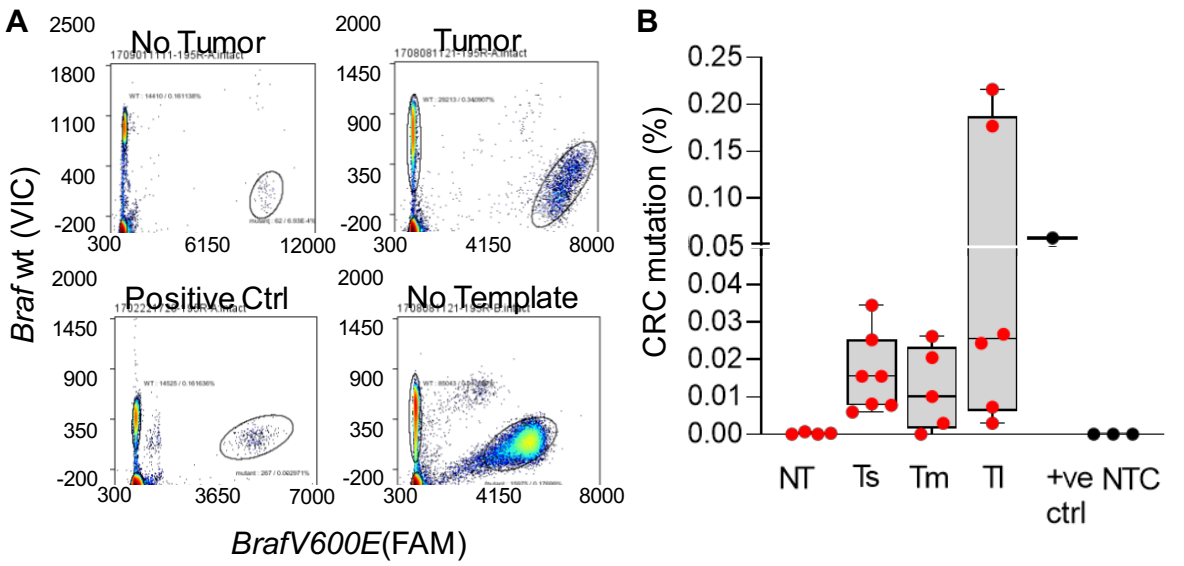

Figure S7: High sensitivity digital droplet PCR (ddPCR) detection of CRC mutation (*BrafV600E*) in stool DNA isolated from tumor-bearing animals. A, Representative images of ddPCR data. **B,** CRC mutation (*BrafV600E)* positive droplets as a % of total droplets. Analysis of no template negative control samples and stool DNA samples from non-tumor bearing animals was used to determine the sensitivity threshold of the assay. +ve ctrl = positive control samples that contains 10% *BrafV600E* gDNA spiked into stool DNA sample from a non-tumor bearing animal, NT = no tumor, Ts = small tumor, Tm = medium tumor, Tl = large tumor, NTC = no template PCR negative control (n=3-4 mice/group).

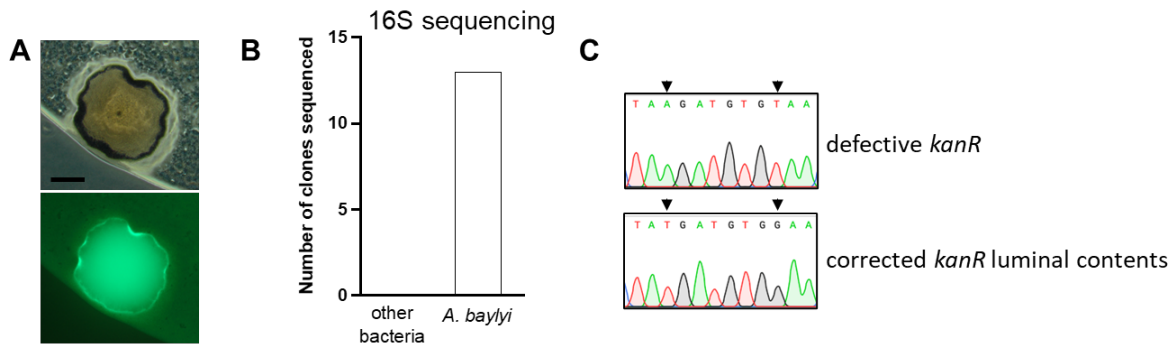

Figure S8: Horizontal gene transfer is detected in luminal contents from mice bearing BTRZI CRC donor tumors after rectal dosing of *A. baylyi* sensor bacteria. Recombined transformants were **A**, GFP positive and confirmed as *A. baylyi* by **B**, 16s sequencing on kanamycin/chloramphenicol/vancomycin selection plates, scale bar 500 µm. **C**, Representative Sanger sequencing chromatograms of PCR amplicon covering the region of the *kanR* gene containing informative SNPs to highlight the difference in sequencing DNA isolated from parental *A. baylyi* sensor bacteria compared to *A. baylyi* colonies isolated from kanamycin/chloramphenicol/vancomycin plates in luminal contents from mice bearing BTRZI CRC donor tumors after rectal dosing of *A. baylyi* sensor bacteria.

Movie S1: *A. baylyi* biosensors taking up plasmid donor DNA.
A. baylyi were grown overnight, washed into fresh LB, mixed with saturating pLenti-KRAS donor DNA, and sandwiched between an agar pad and a glass bottom dish. Images were taken every 10 minutes. GFP fluorescence indicates that the cells have taken up and genomically integrated the donor DNA cassette.

Supplementary Materials References

38. R. M. Cooper, J. Hasty, One-Day Construction of Multiplex Arrays to Harness Natural CRISPR-Cas Systems. *Acs Synth Biol*. **9**, 1129–1137 (2020).

39. S. C. Pearce, R. L. McWhinnie, F. E. Nano, Synthetic temperature-inducible lethal gene circuits in Escherichia coli. *Microbiology+*. **163**, 462–471 (2017).

40. T. R. M. Lannagan, Y. K. Lee, T. Wang, J. Roper, M. L. Bettington, L. Fennell, L. Vrbanac, L. Jonavicius, R. Somashekar, K. Gieniec, M. Yang, J. Q. Ng, N. Suzuki, M. Ichinose, J. A. Wright, H. Kobayashi, T. L. Putoczki, Y. Hayakawa, S. J. Leedham, H. E. Abud, Ö. H. Yilmaz, J. Marker, S. Klebe, P. Wirapati, S. Mukherjee, S. Tejpar, B. A. Leggett, V. L. J. Whitehall, D. L. Worthley, S. L. Woods, Genetic editing of colonic organoids provides a molecularly distinct and orthotopic preclinical model of serrated carcinogenesis. *Gut*. **68**, 684 (2019).

41. T. Sato, D. E. Stange, M. Ferrante, R. G. J. Vries, J. H. van Es, S. van den Brink, W. J. van Houdt, A. Pronk, J. van Gorp, P. D. Siersema, H. Clevers, Long-term Expansion of Epithelial Organoids From Human Colon, Adenoma, Adenocarcinoma, and Barrett's Epithelium. *Gastroenterology*. **141**, 1762–1772 (2011).

42. C. Becker, M. C. Fantini, M. F. Neurath, High resolution colonoscopy in live mice. *Nat Protoc*. **1**, 2900–2904 (2006).

43. K. P. O'Rourke, E. Loizou, G. Livshits, E. M. Schatoff, T. Baslan, E. Manchado, J. Simon, P. B. Romesser, B. Leach, T. Han, C. Pauli, H. Beltran, M. A. Rubin, L. E. Dow, S. W. Lowe, Transplantation of engineered organoids enables rapid generation of metastatic mouse models of colorectal cancer. *Nat Biotechnol*. **35**, 577–582 (2017).